Aging attenuates diurnal lipid uptake by brown adipose tissue

Wietse In het Panhuis[1,2], Milena Schönke[1,2], Ricky Siebeler[1,2], Salwa Afkir[1,2], Rianne Baelde[1,2], Amanda C.M. Pronk[1,2], Trea C.M. Streefland[1,2], Hetty C.M. Sips[1,2], Reshma A. Lalai[1,2], Patrick C.N. Rensen[1,2], Sander Kooijman[1,2]

[1]Division of Endocrinology, Department of Medicine, Leiden University Medical Center, Leiden, The Netherlands
[2]Einthoven Laboratory for Experimental Vascular Medicine, Leiden University Medical Center, Leiden, The Netherlands

Correspondence to: Wietse In het Panhuis; **email:** w.in_het_panhuis@lumc.nl

ABSTRACT

Brown adipose tissue (BAT) contributes to cardiometabolic health by taking up glucose and lipids for oxidation, a process that displays a strong diurnal rhythm. While aging has been shown to reduce thermogenic characteristics of BAT, it is as yet unknown whether this reduction is specific to the time of day. Therefore, we assessed whole-body and BAT energy metabolism in young and middle-aged male and female C57BL/6J mice and studied the consequences for lipid metabolism in humanized APOE*3-Leiden.CETP mice (also on a C57BL/6J background). We demonstrate that in middle-aged versus young mice body temperature is lower in both male and female mice, while uptake of triglyceride (TG)-derived fatty acids (FAs) by BAT, reflecting metabolic activity, is attenuated at its peak at the onset of the dark (wakeful) phase in female mice. This coincided with delayed plasma clearance of TG-rich lipoproteins and TG-depleted lipoprotein core remnants, and elevated plasma TGs at the same time point. Furthermore, middle-aged female mice showed increased adiposity, accompanied by lipid accumulation, increased expression of genes involved in lipogenesis, and reduced expression of genes involved in fat oxidation and the intracellular clock machinery in BAT. Peak abundance of lipoprotein lipase (LPL), a crucial regulator of FA uptake, was attenuated in BAT. Our findings suggest that LPL is a potential therapeutic target for restoring diurnal metabolic BAT activity, and that efficiency of strategies targeting BAT may be improved by including time of day as an important factor.

INTRODUCTION

Aging gradually increases the risk of cardiometabolic diseases through – among others – increased adiposity and elevated plasma lipid levels, starting already in young adulthood [1]. Although the etiology is likely to be multifactorial, an important contributing process is adipose tissue remodeling [2]. Besides an overall increase in adiposity, aging is characterized by higher visceral vs. subcutaneous white adipose tissue (WAT) ratio, and lower thermogenic activity of brown adipose tissue (BAT) [3–5].

Whilst WAT stores nutritional energy as triglycerides (TGs), BAT takes up large amounts of glucose and TG-derived fatty acids (FAs) for oxidation to produce heat. Accordingly, nutrient uptake by BAT can be used as a proxy for its thermogenic activity [6–9], and many favorable cardiometabolic effects have been attributed to BAT activation in mice [10, 11]. The presence of metabolically active BAT in humans is also associated with cardiometabolic health [12, 13], though more prospective studies are needed to establish the causality of this relationship. Interestingly, we and others have demonstrated that both glucose and lipid uptake by BAT is characterized by a high amplitude diurnal oscillation (i.e., rhythms synchronized to a light-dark cycle) [14–19], likely to maintain body temperature during the rest phase and facilitate the rise in body temperature prior to wakening.

Reduced nutrient uptake by BAT may (partly) explain the age-related increase in adiposity and elevated plasma lipid levels. It is, however, unknown if aging causes an overall reduction in nutrient uptake by BAT or a time of day-specific reduction, and whether this has consequences for diurnal rhythms of plasma (postprandial) lipid levels. Insight into age-related changes in diurnal nutrient uptake by BAT may lead to the identification or optimization of strategies to promote nutrient uptake by BAT and improve cardiometabolic health.

In this study, we aimed to assess the consequences of aging on diurnal nutrient uptake in BAT and show that in middle-aged mice lipid uptake is attenuated at its diurnal peak in female but not male C57BL/6J mice, which coincided with elevated plasma lipid levels and increased adiposity in APOE*3-Leiden.CETP mice (on a C57BL/6J background), a well-established mouse model for human lipoprotein metabolism [20, 21].

RESULTS

Aging attenuates body temperature rhythm in male and female wildtype mice, but decreases uptake of lipids by brown adipose tissue in females only

To study the metabolic consequences of aging, young (12 weeks old) and middle-aged (52 weeks old) male and female wildtype mice (C57BL/6J background) were utilized. In both sexes, middle-aged mice had a higher body weight (Supplementary Figure 1A, 1C) than young mice explained by higher lean mass (Supplementary Figure 1B, 1D) and fat mass (Supplementary Figure 1E, 1G), though with an increased body fat percentage (Supplementary Figure 1F, 1H). To evaluate the effects of aging on energy homeostasis; energy intake and energy expenditure (indirect calorimetry, voluntary activity in home cage, and core body temperature) were monitored for 3 days. Despite differences in body weight, there was no difference in voluntary activity (Figure 1A–1D), food intake (Figure 1E–1H), energy expenditure estimated from oxygen consumption and carbon dioxide production (Supplementary Figure 2A–2D) and respiratory exchange ratio (Supplementary Figure 2E–2H) between young and middle-aged mice in both sexes, indicating that middle-aged mice might have an altered substrate partitioning. Indeed, core body temperature was reduced during the light (inactive) phase in middle-aged mice of both sexes (Figure 1I–1L). To assess if this effect could be attributed to altered metabolic activity in adipose tissue, we intravenously injected mice with TG-rich lipoprotein-like particles labeled with glycerol tri[^{3}H]oleate, and 2-[1-^{14}C]-deoxyglucose at the end of the light phase, denoted as

Zeitgeber Time (ZT)12. This time point also corresponds to the previously reported peak in metabolic BAT activity [17], and changes in BAT activity at this time of day are therefore expected to have the biggest metabolic impact. In line with previous experiments, uptake of both radiolabels was higher in BAT than in WAT independent of sex (Figure 1M–1T), and BAT showed higher metabolic activity in females than in males regardless of age, although we could not formally test as the sexes were treated as separate cohorts. In middle-aged male mice, [^{3}H]oleate uptake by interscapular (i)BAT and subscapular (s)BAT was non-significantly reduced when compared to young male mice (Figure 1M). Uptake of [^{3}H]oleate by subcutaneous (s)WAT but not gonadal (g)WAT was lower in middle-aged male mice compared with young male mice. In middle-aged female mice, [^{3}H]oleate uptake by the BAT depots was significantly lower, and also uptake by sWAT and gWAT was lower compared with young mice (Figure 1O). Interestingly, 2-[1-^{14}C]-deoxyglucose uptake by BAT and WAT was unchanged between young and middle-aged mice of both sexes (Figure 1N, 1P, 1R, 1T), illustrating tissue and substrate-specific alterations in nutrient handling during aging. Collectively, these data show that specifically in females aging decreases the uptake of lipids by BAT as measured at the onset of the dark phase.

Aging attenuates processing of triglyceride-rich lipoproteins in APOE*3-Leiden.CETP mice at peak activity of brown adipose tissue

To determine whether the reduction in TG-derived FA uptake by BAT and WAT in aged female mice is caused by a time of day-specific decrease or an overall decrease in metabolic activity of the tissue, we performed a new study comparing lipid handling at the end of the light phase (ZT12) and dark phase (ZT0), corresponding to peak and nadir TG-derived FA uptake by BAT [17], as a proxy for diurnal uptake. This time we utilized female APOE*3-Leiden.CETP mice (also on a C57BL/6J background), which is a well-established mouse model for human lipoprotein metabolism, to simultaneously address lipid uptake by BAT and the clearance of TG-depleted lipoprotein core remnants by the liver. Body weight and composition were monitored over 16 weeks while the mice were fed a cholesterol-enriched Western-type diet (25% kJ from fat) to induce hyperlipidemia, starting at the age of 11–15 weeks in young mice and 51–55 weeks in middle-aged mice. Throughout this period, compared to young mice, middle-aged mice consistently showed higher body weight (Supplementary Figure 3A) due to higher lean mass (Supplementary Figure 3B) and fat mass (Supplementary Figure 3C), as well as a higher body fat percentage (Supplementary Figure 3D). Food intake was higher in middle-aged mice

than young mice (Supplementary Figure 3E), but lower when expressed relative to body weight (Supplementary Figure 3F), and unchanged when adjusted for lean mass (Supplementary Figure 3G).

At the endpoint, plasma clearance and organ uptake of glycerol tri[^{3}H]oleate and [^{14}C]cholesteryl oleate from intravenously injected TG-rich lipoprotein-like particles were assessed. In WAT and skeletal muscles
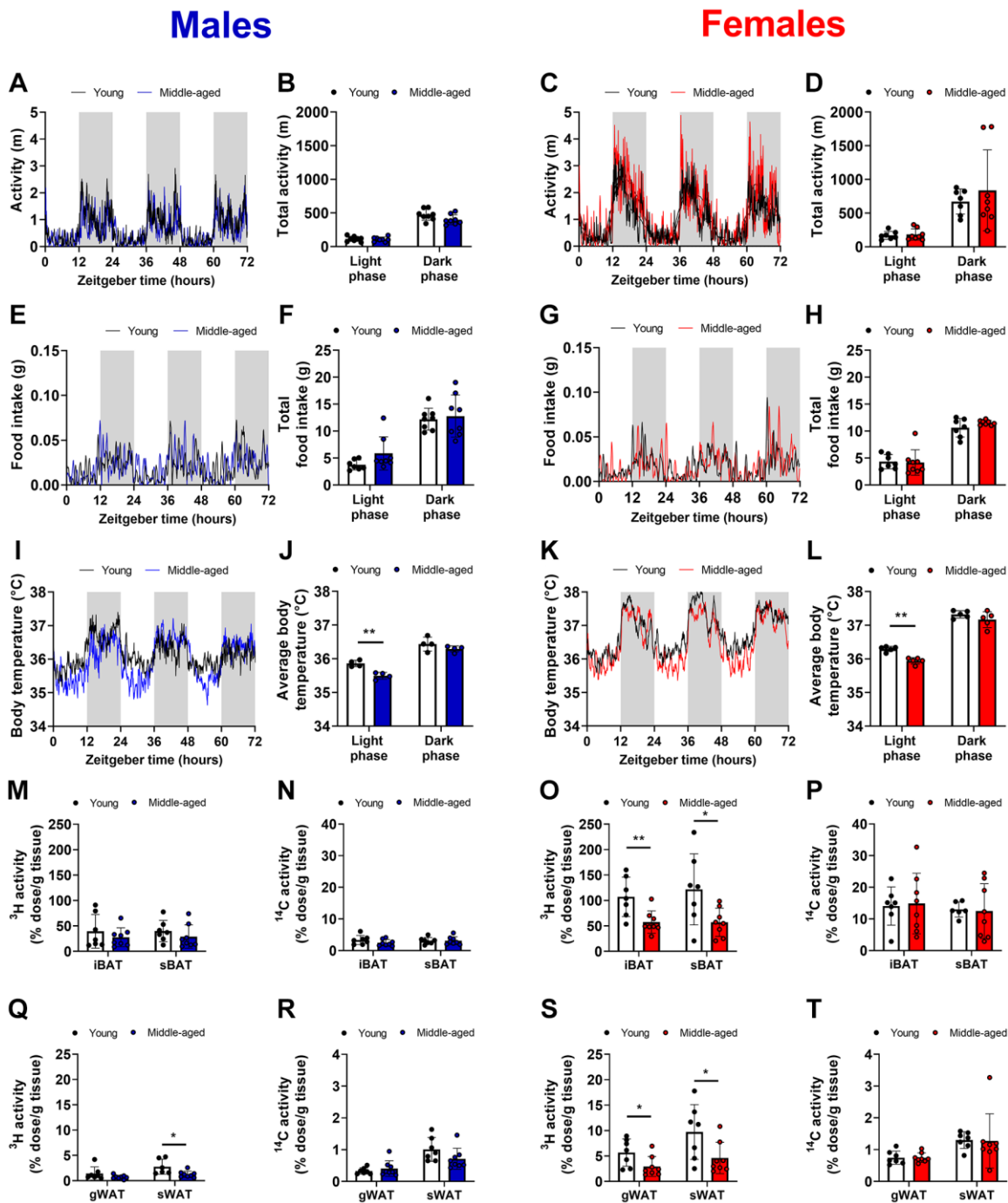

Figure 1. Voluntary activity, food intake, core body temperature, and triglyceride-derived fatty acid uptake by brown and white adipose tissue during aging. Young (12 weeks old) and middle-aged (52 weeks old) male (left panels in blue) and female (right panels in red) C57BL/6J mice were single-housed in metabolic home-cages for continuous measurement of (**A–D**) voluntary locomotor activity (n = 7–8 mice/group), (**E–H**) food intake (n = 7–8 mice/group), and (**I–L**) core body temperature with implanted telemetric probes (n = 5 mice/group). Mice were injected with triglyceride-rich lipoprotein-like particles labeled with glycerol tri[^{3}H]oleate and 2-[1-^{14}C]-deoxyglucose at *Zeitgeber* Time 12 to assess uptake of the radiolabels by interscapular brown adipose tissue (iBAT) and subscapular BAT (sBAT) (**M–P**) and by gonadal white adipose tissue (gWAT) and subcutaneous WAT (sWAT) (**Q–T**) (n = 6–8 mice/group). Bar graphs represent means ± SD. *p < 0.05; **p < 0.01, according to unpaired *t*-test or two-way ANOVA and following Šídák's multiple-comparison test.

(i.e., extensor digitorum longus, tibialis anterior, and soleus), [³H]oleate uptake, reflecting TG-derived FA uptake, was not different between ZT12 and ZT0 in young mice and lowered in middle-aged mice (Supplementary Figure 4). In contrast, [³H]oleate uptake by iBAT, sBAT, and perivascular adipose tissue (pVAT) was 3-fold higher at ZT12 compared with ZT0 in young mice, while [³H]oleate uptake in middle-aged mice was not oscillating (Figure 2A–2C). Notably, [³H]oleate uptake by the BAT depots in the older mice was not different from the anticipated nadir at ZT0 in young mice (Figure 2A–2C), indicating a time of day-specific reduction rather than a total reduction in activity (time-age interaction by two-way ANOVA: $P = 0.033$,
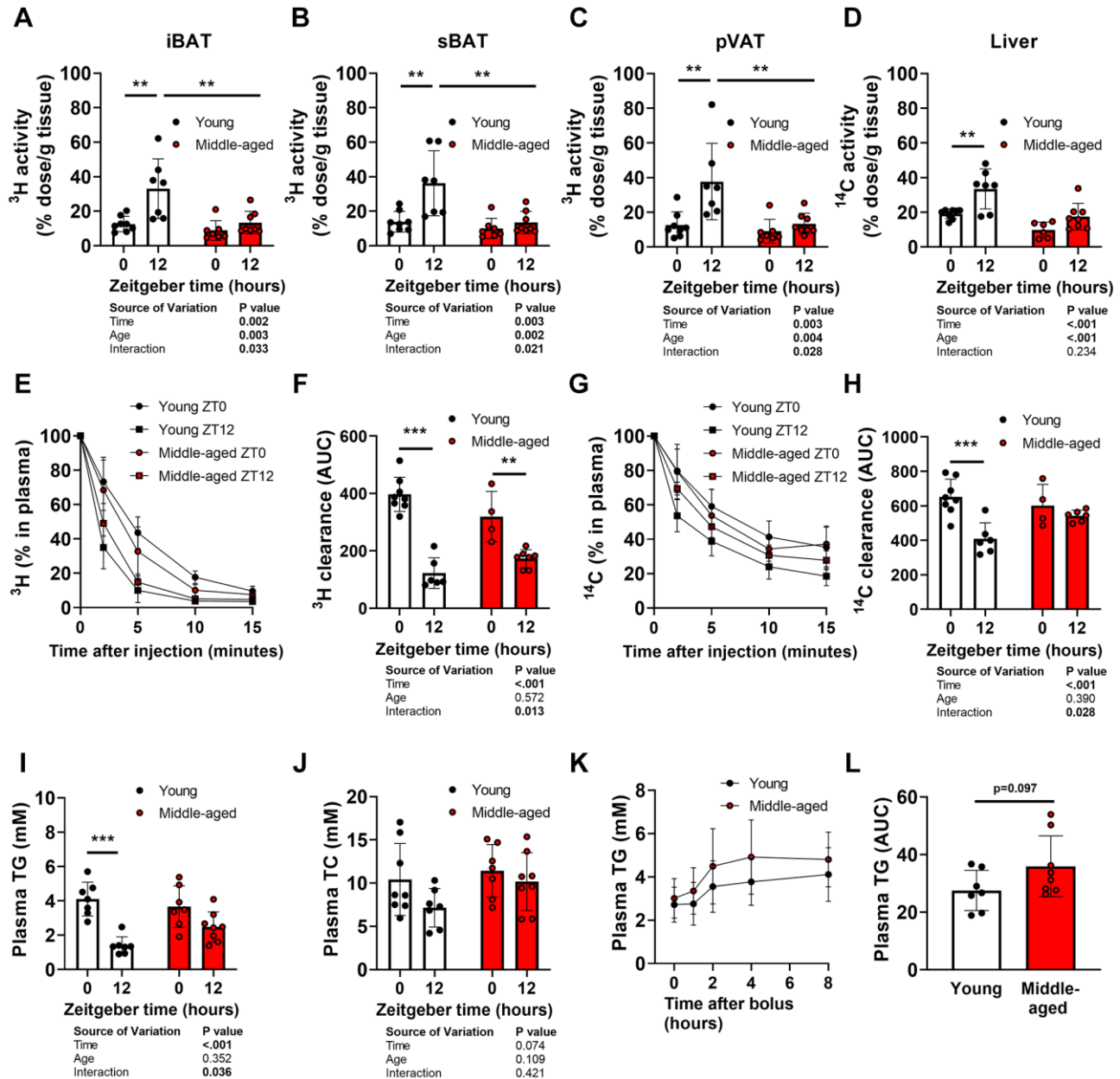

Figure 2. Oscillations of organ uptake, plasma clearance, and plasma levels of lipids during aging. Young (27–31 weeks old) and middle-aged (67–71 weeks old) female APOE*3-Leiden.CETP mice were injected with triglyceride (TG)-rich lipoprotein-like particles double-labeled with glycerol tri[³H]oleate and [¹⁴C]cholesteryl oleate at *Zeitgeber* Time 0 and 12 (n = 7–8 mice/group/time point) to assess [³H]oleate uptake by (**A**) interscapular brown adipose tissue (iBAT), (**B**) subscapular BAT (sBAT), and (**C**) perivascular adipose tissue (pVAT), and (**D**) [¹⁴C]cholesteryl oleate uptake by the liver, and plasma decay of (**E**, **F**) [³H]oleate and (**G**, **H**) [¹⁴C]cholesteryl oleate (n = 4–8 mice/group/time point). Fasted plasma levels of (**I**) TG and (**J**) total cholesterol (TC) (n = 7–8 mice/group/time point). (**K**) Oral lipid tolerance test performed at ZT12 with blood collection for plasma TG measurement, after which (**L**) the area under the curve (AUC) was calculated (n = 7–8 mice/group). Bar graphs and data points on curves represent means ± SD. *p < 0.05; **p < 0.01; ***p < 0.001, according to unpaired t-test or two-way ANOVA and following Tukey's multiple-comparison test.

$P = 0.021$, and $P = 0.028$ for respectively iBAT, sBAT, and pVAT). [14C]cholesteryl oleate uptake by the liver, reflecting the clearance of delipidated lipoprotein remnants, was higher at ZT12 compared with ZT0 in young mice, but not in middle-aged mice. Interestingly, [14C]cholesteryl oleate uptake by the liver was decreased by age, regardless of time of day (age effect by two-way ANOVA: $P < 0.001$) (Figure 2D).

In line with the higher TG-derived FA uptake by BAT and hepatic uptake of TRL-remnants at ZT12 compared to ZT0 in young mice, plasma decay of [3H]- and [14C]-derived activity was faster at ZT12 than at ZT0 in young mice (Figure 2E–2H). In contrast, these differences were attenuated in middle-aged mice (time-age interaction by two-way ANOVA: $P = 0.013$ and $P = 0.028$ for respectively [3H]oleate and [14C]cholesteryl oleate decay; significant differences between groups at individual time points not shown). The diurnal variation in the ability to clear plasma lipids was accompanied by a diurnal variation in plasma TG levels in young, but not middle-aged mice (Figure 2I). Total cholesterol levels were not different at ZT12 vs. ZT0 regardless of age (Figure 2J). Postprandial TG excursions following

an oral lipid tolerance test with a fixed amount of olive oil at ZT12 tended to be elevated in middle-aged mice ($P = 0.097$; Figure 2K, 2L).

Aging promotes whitening of brown adipose tissue in female APOE*3-Leiden.CETP mice

To investigate mechanisms underlying time of day-specific reductions in TG-derived FA uptake by BAT during aging, morphology and markers of BAT function in tissues collected from female APOE*3-Leiden.CETP mice at ZT0 and ZT12 were analyzed. Middle-aged mice showed greater iBAT (Figure 3A) and sBAT (Figure 3B) mass compared with young mice, but not when expressed relative to body weight (Figure 3C, 3D). In line with a higher body fat percentage, histological analysis of lipid content of sBAT showed increases in middle-aged mice (age effect by two-way ANOVA: $P = 0.003$) (Figure 3E), indicating whitening of the tissue.

To investigate if attenuated diurnal BAT activity during aging coincides with changes in the cellular clock machinery, a major driving force behind cellular oscillations, expression of several clock genes was
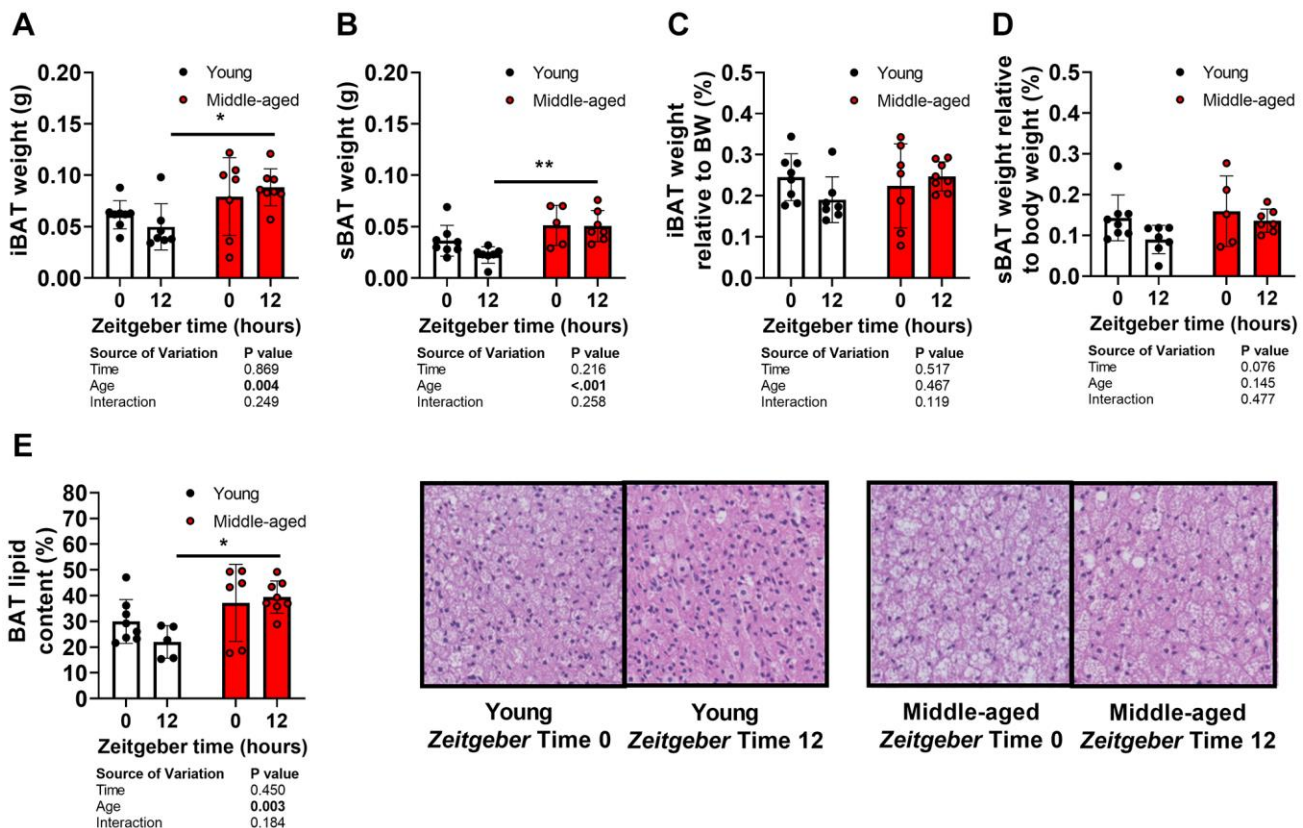

Figure 3. Brown adipose tissue morphology and aging. Tissues of young (27–31 weeks old; white circles) and middle-aged (67–71 weeks old; black circles) female APOE*3-Leiden.CETP mice were collected at *Zeitgeber* Time 0 and 12 ($n = 7$–8 mice/group/time point). (**A**) interscapular brown adipose tissue (iBAT) and (**B**) subscapular BAT (sBAT) were weighed, and (**C**, **D**) expressed as percentage of body weight ($n = 5$–8 mice/group/time point). (**E**) Lipid content of sBAT was quantified and representative pictures are shown ($n = 5$–8/group/time point). Bar graphs represent means ± SD. $^*p < 0.05$; $^{**}p < 0.01$, according to two-way ANOVA and following Tukey's multiple-comparison test.

measured in BAT. Whilst patterns for time-dependent expression of circadian locomotor output cycles kaput (*Clock*), period 1 (*Per1*), cryptochrome 1 (*Cry1*), nuclear receptor subfamily 1 group D member 1 (*Nr1d1*, encoding REV-ERBA), and brain and muscle ARNT-like 1 (*Bmal1*) were not different (Figure 4A–4E),
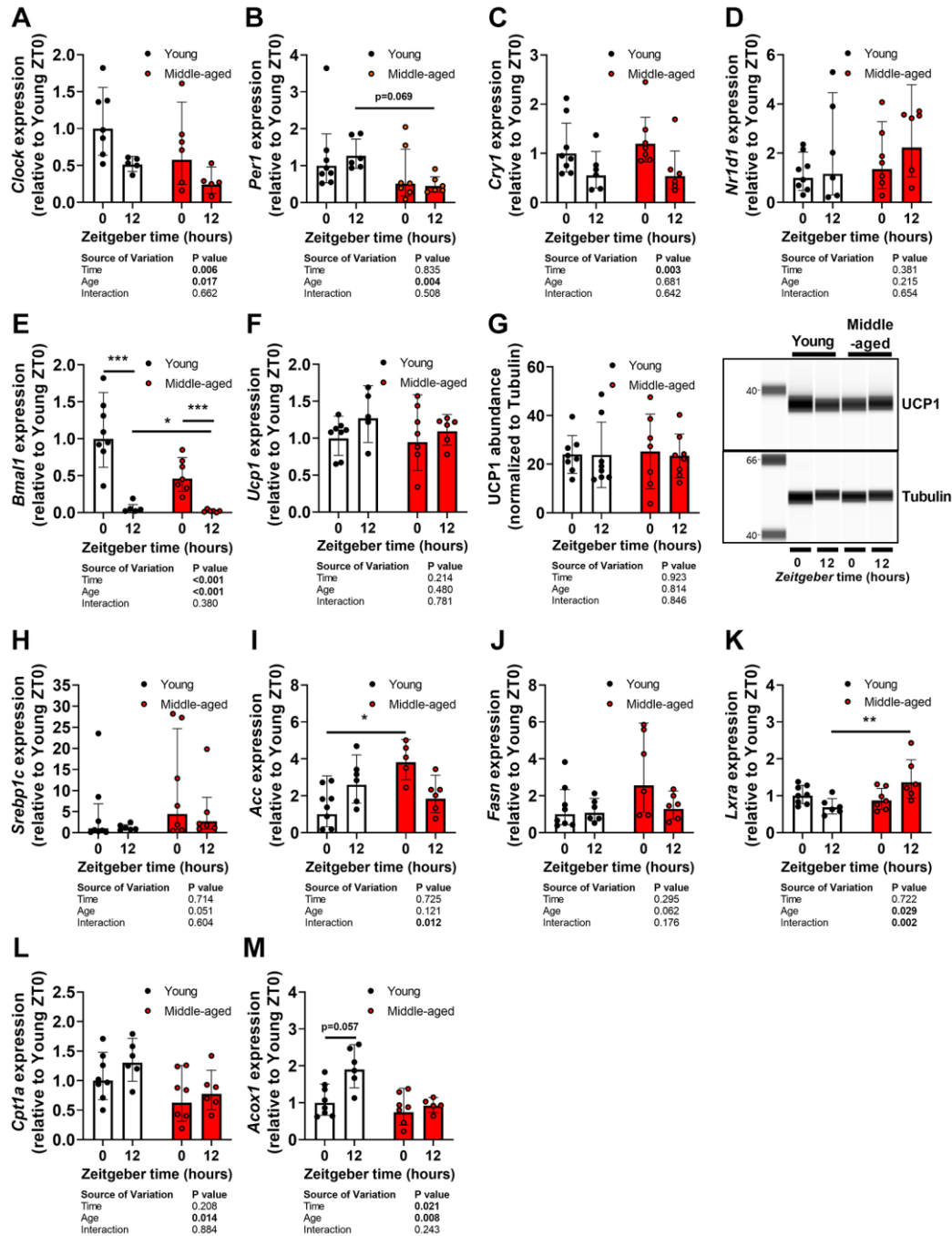

Figure 4. Lipogenesis, beta-oxidation, and the cellular clock in brown adipose tissue during aging. Subscapular brown adipose tissue of young (27–31 weeks old; white circles or bars) and middle-aged (67–71 weeks old; black circles or bars) female APOE*3-Leiden.CETP mice was collected at *Zeitgeber* Time 0 and 12 (n = 7–8 mice/group/time point). Gene expression of (**A**) circadian locomotor output cycles kaput (*Clock*), (**B**) period 1 (*Per1*), (**C**) cryptochrome 1 (*Cry1*), (**D**) *Nr1d1* (REV-ERBA)*,* (**E**) brain and muscle ARNT-like 1 (*Bmal1*), and (**F**) uncoupling protein 1 (*Ucp1*) as determined by quantitative polymerase chain reaction, normalized to *ß-actin*, and shown relative to the expression in young mice at ZT0 (n = 5-8 mice/group/time point). (**G**) Protein abundance of UCP1 as measured by automated Western blotting, and normalized to Tubulin levels (n = 7–8 mice/group/time point). Gene expression of (**H**) sterol regulatory element-binding protein 1c (*Srebp1c*), (**I**) acetyl-CoA carboxylase (*Acc*), (**J**) fatty acid synthase (*Fasn*), (**K**) liver X receptor alpha (*Lxra*), (**L**) carnitine palmitoyltransferase 1a (*Cpt1a*), and (**M**) peroxisomal acyl-coenzyme A oxidase 1 (*Acox1*). Bar graphs represent means ± SD. $^*p$ < 0.05; $^{**}p$ < 0.01, $^{***}p$ < 0.001, according to two-way ANOVA and following Tukey's multiple-comparison test.

middle-aged mice showed reduced expression of *Clock*, *Per1*, and *Bmal1* when compared to young mice (age effect by two-way ANOVA: $P = 0.017$, $P = 0.004$, and $P < 0.001$, for respectively *Clock*, *Per1*, and *Bmal1*).

Next, we assessed markers of thermogenesis, lipogenesis, and beta oxidation in the same tissues. Gene expression (Figure 4F) and protein abundance (Figure 4G) of uncoupling protein 1 (UCP1) were not different between ZT0 and ZT12, or affected by age. Expression of lipogenic genes sterol regulatory element-binding protein 1c (*Srebp1c*) (Figure 4H), acetyl-CoA carboxylase (*Acc*) (Figure 4I), and fatty acid synthase (*Fasn*) (Figure 4J) tended to be increased in middle-aged mice (age effect by two-way ANOVA: $P = 0.051$, $P = 0.121$, and $P = 0.062$, for *Srebp1c*, *Acc*, and *Fasn*, respectively). In addition, expression of liver X receptor alpha (*Lxra*) (Figure 4K), a negative regulator of beta-oxidation in BAT [22], was significantly increased at ZT12 in middle-aged mice compared with young mice. Accordingly, gene expression of *Cpt1a* (Figure 4L),

encoding a crucial factor for FA transport into mitochondria prior to beta oxidation [23], and peroxisomal acyl-coenzyme A oxidase 1 (*Acox1*) (Figure 4M), encoding an enzyme involved in beta oxidation, was reduced in middle-aged mice (age effect by two-way ANOVA: $P = 0.014$ and $P = 0.008$, for respectively *Cpt1a* and *Acox1*). These data suggest altered functioning of BAT with an increase in lipogenesis and reduction in fat oxidation, but do not explain the attenuated lipid uptake by the tissue.

Aging attenuates lipoprotein lipase expression and abundance in brown adipose tissue of female APOE*3-Leiden.CETP mice

We next assessed expression of *Lpl* and its negative regulator *Angptl4* in BAT, as we have previously shown that these are crucial regulators of diurnal TG-derived FA uptake [17, 24]. *Lpl* gene expression (Figure 5A) and LPL protein abundance (Figure 5B) were higher at ZT12 than ZT0 in young mice, in line with previous
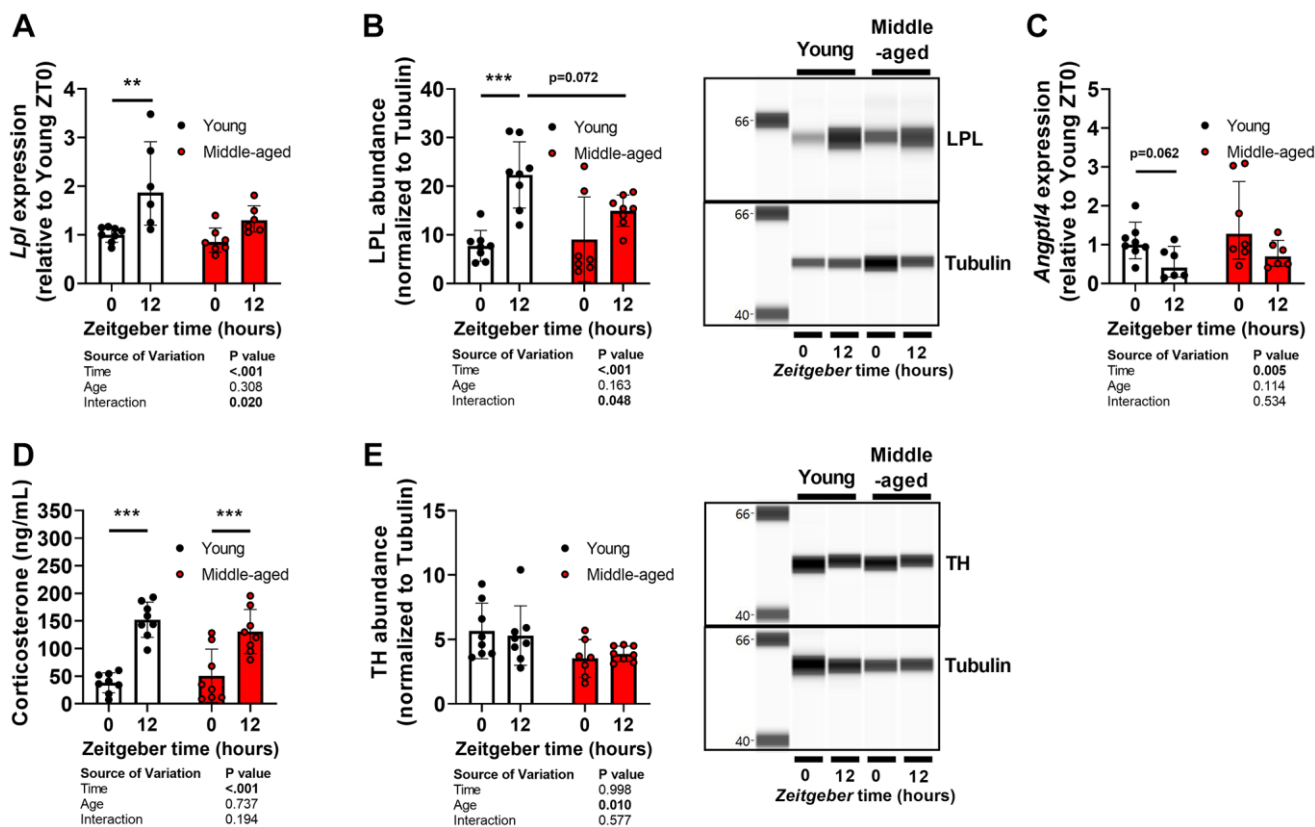

Figure 5. Oscillations of lipoprotein in brown adipose tissue and its regulators during aging. Subscapular brown adipose tissue of young (27–31 weeks old; white circles or bars) and middle-aged (67–71 weeks old; black circles or bars) female APOE*3-Leiden.CETP mice was collected at *Zeitgeber* Time 0 and 12 (*n* = 7–8 mice/group/time point). (**A**) Gene expression of lipoprotein lipase (*Lpl*) measured by quantitative polymerase chain reaction, normalized to *ß-actin*, and shown relative to the expression in young mice at ZT0. (**B**) Protein abundance of LPL measured by automated Western blot, and normalized to Tubulin levels. (**C**) Gene expression of angiopoietin-like 4 (*Angptl4*). (**D**) Corticosterone levels measured in plasma collected from young (17–21 weeks old) and middle-aged (57–61 weeks old) mice at *Zeitgeber* Time 0 and 12. (**E**) Protein abundance of tyrosine hydroxylase (TH). Bar graphs represent means ± SD. **p < 0.01; ***p < 0.001, according to two-way ANOVA and following Tukey's multiple-comparison test.

observations [17, 24], but not in middle-aged mice. *Angptl4* expression tended to be lower at ZT12 than ZT0 regardless of age (Figure 5C).

We previously also demonstrated involvement of glucocorticoids and the sympathetic nervous system in the diurnal control of BAT activity including the regulation of LPL and ANGPTL4 activity [14, 17]. However, corticosterone levels were not different between young and middle-aged mice (Figure 5D). Protein abundance of tyrosine hydroxylase (TH) (Figure 5E), the rate-limiting enzyme in the synthesis of noradrenalin and a marker of sympathetic activity, was reduced in middle-aged mice (age effect by two-way ANOVA: $P = 0.012$). However, TH abundance was not different between ZT0 and ZT12 in young or middle-aged mice.

DISCUSSION

BAT displays pronounced diurnal variation in transcriptional activity, lipid content, and nutrient uptake [17, 18, 24, 25], of which the latter highly contributes to the beneficial effects of BAT on cardiometabolic health [10, 11]. While previous studies show an age-related dampening in oscillations of mRNA levels and lipid abundance in BAT [25, 26], it is unknown how aging affects diurnal nutrient uptake by BAT. Here we demonstrated that with age this rhythm of nutrient uptake is attenuated characterized by a selective reduction in TG-derived FA uptake at the onset of the dark phase in specifically female mice, an effect that was accompanied by elevated plasma lipid levels and by adipose tissue remodeling.

In females, metabolic activity of BAT is generally higher than in males probably because females can rely to a lesser extent on thermogenesis by skeletal muscle [27]. The age-related reduction in TG-derived FA uptake may therefore be more pronounced and picked up at an earlier age in females compared to males. This is likely because previous studies have reported overall reductions in thermogenic characteristics based on glucose uptake, morphology, and mRNA and protein levels in BAT [3–5] in both sexes at far higher age of 2 years and older. Similarly, the fact that we studied middle-aged rather than old mice may also explain why uptake of TG-derived FAs, but not glucose, was decreased in middle-aged female C57BL/6J mice, since aging has often been reported to reduce glucose uptake by BAT in mice and humans [3, 6, 28]. As thermogenesis in BAT is particularly dependent on FA oxidation rather than glucose oxidation [29, 30], it is possible that reductions in TG-derived FA uptake precede reductions in glucose uptake during aging.

We subsequently assessed the consequences of attenuated TG-derived FA uptake by BAT on lipoprotein metabolism in Western-type diet-fed APOE*3-Leiden.CETP mice. To be able to do so independent of the age-related changes in very-low-density-lipoprotein-cholesterol secretion from the liver [31], we decided to increase the cholesterol content of the diet for the middle-aged APOE*3-Leiden.CETP mice so that plasma cholesterol levels were comparable between groups. The relatively low fat content (25 kJ% fat) is not expected to induce altered circadian rhythms as reported for classical high fat diets (45-60 kJ% fat), but we cannot fully exclude an age-diet interaction. In this context, we observed that attenuated TG-derived FA uptake by BAT at the onset of the dark phase, corresponding with the peak in daily activity, resulted in elevated plasma (postprandial) TG levels and reduced hepatic uptake of TRL-remnants. Involvement of other metabolic tissues in the attenuated ZT0-ZT12 differences in lipoprotein metabolism cannot be excluded, but may be limited as BAT is the metabolic organ with the most pronounced diurnal oscillations in lipid uptake [17]. These observations in mice are very comparable to what we and others have previously reported for humans, with dampened rhythms of plasma lipid levels and impaired postprandial lipid handling in the early wake phase in aged individuals [1, 32, 33]. We anticipate that the de-regulation of these oscillations impairs cardiometabolic health [34, 35].

Mechanistically, aging caused a time-age interaction, with a trend for lower LPL abundance at ZT12, a factor which we previously identified as crucial regulator of diurnal metabolic BAT activity [17, 24] driven by rhythmic activity of glucocorticoids and possibly the sympathetic nervous system [14, 36]. In the current study we did not find evidence for altered glucocorticoid levels or oscillations; an effect that is expected at higher age in C57BL/6J mice [37, 38]. We observed a reduction in abundance of sympathetic activity marker TH, although this should be interpreted with caution as it was not significantly different between ZT0 and ZT12 in young mice. Previous findings showed attenuations in both oscillations of glucocorticoids and sympathetic stimulation and signaling in BAT in mice and humans during aging [39–41], indicating that these factors may influence diurnal BAT activity at older ages. Interestingly, we did observe reduced expression of clock genes in BAT of mice at middle-age. Regular expression of clock genes is important for metabolic health as mutations in humans and knockout in mice promote cardiometabolic disease [42]. In line with our observations that middle-aged mice show reduced *Bmal1* expression, loss of *Bmal1* in BAT has been shown to result in reduced beta oxidation and to promote whitening of BAT [43]. Given

that nearly half of the transcriptome of BAT is oscillating with distinctive expression patterns [24], future studies should include more time points to delineate mechanisms underlying the age-related attenuation of diurnal metabolic BAT activity.

The million-dollar question is how to prevent or reverse aging-associated diseases. Several strategies have shown to be effective in improving the age-related decline in total BAT activity, such as exercise [44], caloric restriction [45], cold exposure [46], and orexin [47]. Our observation that aging reduces lipid uptake by BAT particularly at its peak suggests that efficiency of strategies targeting BAT can be improved by including time of day as an important factor. We additionally postulate LPL as a potential therapeutic target for restoring diurnal metabolic BAT activity from middle-age onwards, and various novel strategies to regulate LPL expression and activity are currently under development [48].

METHODS

Animals

All experiments were performed in accordance with the Institute for Laboratory Animal Research Guide for the Care and Use of Laboratory Animals and were approved by the National Committee for Animal experiments. All mice were housed in groups of 2–4 mice per cage under standard conditions with 12:12 hour light-dark cycles at 21°C with *ad libitum* access to water and diet, unless indicated otherwise. In the first experiment, young (12 weeks old) and middle-aged (52 weeks old) male C57BL/6JRj (Janvier Labs, Le Genest-Saint-Isle, France) and female C57BL/6J (Charles River Laboratories, Wilmington, MA, USA) ($n = 8$ mice per group) were fed a chow diet (Rat and Mouse No.3 Breeding; SDS, Horley, United Kingdom) and 4–5 mice from each group were subcutaneously implanted a telemetry transmitter (Sable Systems GmbH, Berlin, Germany) to measure body temperature. After 3 weeks, mice were killed at the onset of the dark phase (ZT12) to assess organ uptake of TG-derived FAs and glucose (see below in the section 'Clearance of radiolabeled TG-rich lipoprotein-like emulsion particles'). In a second experiment, young (9–13 weeks old) and middle-aged (49–53 weeks old) female APOE*3-Leiden.CETP mice were utilized ($n = 16$ mice per group). APOE*3-Leiden.CETP mice were generated as previously described [21]. Young mice received a diet enriched with 0.10% cholesterol and middle-aged mice a diet enriched with 0.30% cholesterol (both containing 16% fat; Diet T; Ssniff-Spezialdiäten GmbH, Soest, Germany). After a dietary run-in period of 3 weeks, baseline measurements were taken and the animals were

followed for 16 weeks to monitor body weight and body composition (EchoMRI 100-Analyzer; EchoMRI, Houston, TX, USA). At week 6, stress-minimized blood was collected in half of the mice at the onset of the light phase (ZT0) and the onset of the dark phase (ZT12) by collecting blood within 2 minutes after lifting the cage to measure plasma corticosterone. At week 8, half of the mice were subjected to a postprandial lipid tolerance test at ZT12. At the end of the study, half of the young (27–31 weeks old) and middle-aged (67–71 weeks old) mice in each group was killed at ZT0 and the other half at ZT12 to assess plasma lipid levels as well as plasma decay and organ uptake of TG-derived FAs and TRL-remnants.

Body temperature and indirect calorimetry

A telemetric transmitter (weight, 1.1 g; volume, 0.52 mL; G2 E-mitter, Starr, Elst, The Netherlands) was implanted into the abdominal cavity after which the mice were allowed to recover for 2 weeks before they were individually housed in automated metabolic home cages (Promethion System; Sable Systems, Las Vegas, NV, USA) for another 5 days. The first 2 days were considered as acclimatization phase and were not included in the data analysis. Voluntary locomotor behavior (by infrared beam breaks), food intake, body temperature, O_2 consumption, and CO_2 production were continuously collected in 5 minute bins and energy expenditure and respiratory exchange ratio were calculated. Energy expenditure was not normalized to lean body mass.

Clearance of radiolabeled TG-rich lipoprotein-like emulsion particles

Mice received an intravenous injection with an emulsion of TRL-like particles (80 nm) containing glycerol tri[^{3}H]oleate (1 mg TG in 200 μL saline per mouse), prepared as described previously [49]. In experiment 1, 2-[1-^{14}C]-deoxyglucose (NEC495A250UC; PerkinElmer, Waltham, MA, USA) was added to the emulsion to assess uptake of glucose and in experiment 2, TRL-like particles were double-labelled with [^{14}C]cholesteryl oleate in addition to glycerol tri[^{3}H]oleate to allow for TRL-remnant clearance. Blood was collected to determine plasma decay of radiolabels. After 15 minutes, mice were killed by CO_2 inhalation and perfused via the heart with ice-cold PBS. Various organs were collected and dissolved in 0.5 mL Solvable (6NE9100, PerkinElmer, Waltham, MA, USA) at 56°C overnight, after which 5.0 mL Ultima Gold (6013329, PerkinElmer, Waltham, MA, USA) was added. Plasma was directly added to 2.5 mL Ultima Gold. ^{3}H-activity and ^{14}C-activity were measured with a scintillation counter

(Tri-Carb 2910 TR, PerkinElmer, Waltham, MA, USA) and expressed as a percentage of injected dose per gram tissue or as a percentage of injected dose in plasma. Mice were excluded from the calculation of the AUC (between 2 and 15 minutes after injection) of plasma decay if one or more plasma samples were missing.

Plasma measurements

Plasma corticosterone levels were measured with Corticosterone HS (High Sensitivity) enzyme immunoassay kit (AC-15F1; Immunodiagnostic Systems Holdings Ltd, Boldon, UK), according to the manufacturer's protocols. Plasma TG and TC levels were measured in plasma collected at week 16 by using Cobas Triglycerides (106571) and Cobas Total Cholesterol (106570) enzymatic kits (both from Roche Diagnostics, Mannheim, Germany), by adding 200 µL reagent (undiluted for TG and $3\times$ diluted for TC) to 2.5 µL sample and incubating at room temperature for 30 min prior to measuring at 492 nm versus 650 nm (for TG) or at 505 nm versus 650 nm (for TC).

Postprandial lipid tolerance

The animals were fasted for 4 hours prior to receiving an olive oil bolus (200 µL per mouse) (Carbonell, Cordoba, Spain) by oral gavage. Tail vein blood was sampled prior to and 1, 2, 4, and 8 hours post-gavage to measure plasma TG levels.

Histology

Paraffin-embedded sBAT (approx. 5–10 mg) from mice of experiment 2 was cross-sectioned (5 µm) and stained with Mayer's hematoxylin (109249, Sigma Aldrich, Saint Louis, MO, USA) and eosin using standard protocols [50]. Lipid content was assessed by quantifying the unstained areas representing intracellular lipid vacuoles using ImageJ software, version 1.52a (National Institutes of Health, Bethesda, MD, USA).

Protein quantification

Frozen sBAT samples (approx. 5 mg) from mice of experiment 2 were lysed in RIPA buffer (150 mM sodium chloride, 1.0% Triton X-100, 0.5% sodium deoxycholate, 0.1% sodium dodecyl sulphate, 50 mM Tris pH 8.0, protease and phosphatase inhibitors (A32959, Thermo Fisher Scientific, Waltham, MA, USA), homogenized by a FastPrep-24™ 5G bead beating grinder and lysis system (4.0 m/s for 10 sec; MP Biomedicals™, Santa Ana, CA, USA) and centrifuged

repeatedly (16.2 g for 5 min at 4°C) to remove fat. Protein concentrations were determined using the Pierce™ BCA Protein Assay Kit (23225, Thermo Fisher Scientific, Waltham, MA, USA), according to manufacturer's protocol. Protein abundance was assessed by automated Western blot using Wes™ (ProteinSimple, Santa Clara, CA, USA) using a rabbit anti-mouse UCP1 antibody (1:20; U6382, Sigma Aldrich, Saint Louis, MO, USA), a goat anti-mouse LPL antibody (1:50; kind gift from André Bensadoun [51]), and a rabbit anti-mouse TH antibody (1:50; ab137869, Abcam, Cambridge, United Kingdom). A rabbit anti-mouse Tubulin antibody (1:10; 2148, Cell Signaling, Danvers, MA, USA) was used for normalization. Protein lysates of 0.02, 0.80, 0.20, and 0.80 µg/µL were used for UCP1, LPL, TH, and Tubulin, respectively. An anti-goat antibody (DM-006, ProteinSimple, Santa Clara, CA, USA) was used for LPL and an anti-rabbit antibody (DM-001, ProteinSimple, Santa Clara, CA, USA) was used for UCP1, TH, and Tubulin. Relative normalized protein levels were quantified by Compass software (ProteinSimple; v5.0.1).

Gene expression analysis

RNA was isolated from frozen sBAT (approx. 5 mg) from mice of experiment 2 by lysing and homogenization using TriPure RNA Isolation Reagent (11667165001, Sigma Aldrich, Saint Louis, MO, USA) and a FastPrep-24™ 5G bead beating grinder and lysis system (4.0 m/s for 10 sec; MP Biomedicals™, Santa Ana, CA, USA). cDNA was synthesized from 1 µg RNA using M-MLV Reverse Transcriptase (M1705, Promega, Madison, WI, USA) and qPCR was conducted utilizing SYBR green kit (Promega, Madison, WI, USA) and a CFX96 PCR machine (Bio-Rad, Hercules, CA, USA), according to the manufacturers' protocols. Gene expression was normalized to β-actin and expressed relative to the Young ZT0 group. Primer sequences are displayed in Supplementary Table 1. Several mice were excluded due to technical errors.

Statistical analyses

$P < 0.05$ was considered statistically significant. Statistical analyses between groups were performed with unpaired t-tests or two-way ANOVA with post-hoc tests, where applicable. Šídák's multiple-comparison test was used in experiment 1 to compare young vs. middle-aged mice within but not between diurnal phases. Tukey's multiple-comparison test was used in experiment 2 to compare young vs. middle-aged mice within time points, as well as ZT0 vs. ZT12. Statistical analyses were performed with GraphPad Prism software, version 9.0.1

(GraphPad, La Jolla, CA, USA). Data are presented as means ± SD.

AUTHOR CONTRIBUTIONS

CONFLICTS OF INTEREST

ETHICAL STATEMENT

All experiments were performed in accordance with the Institute for Laboratory Animal Research Guide for the Care and Use of Laboratory Animals and were approved by the National Committee for Animal experiments.

FUNDING

REFERENCES

1. Liu HH, Li JJ. Aging and dyslipidemia: a review of potential mechanisms. Ageing Res Rev. 2015; 19:43–52.
https://doi.org/10.1016/j.arr.2014.12.001
PMID:25500366

2. Von Bank H, Kirsh C, Simcox J. Aging adipose: Depot location dictates age-associated expansion and dysfunction. Ageing Res Rev. 2021; 67:101259.
https://doi.org/10.1016/j.arr.2021.101259
PMID:33515751

3. Zoico E, Rubele S, De Caro A, Nori N, Mazzali G, Fantin F, Rossi A, Zamboni M. Brown and Beige Adipose Tissue and Aging. Front Endocrinol (Lausanne). 2019; 10:368.
https://doi.org/10.3389/fendo.2019.00368
PMID:31281288

4. Graja A, Gohlke S, Schulz TJ. Aging of Brown and Beige/Brite Adipose Tissue. Handb Exp Pharmacol. 2019; 251:55–72.
https://doi.org/10.1007/164_2018_151
PMID:30141100

5. Dong M, Lin J, Lim W, Jin W, Lee HJ. Role of brown adipose tissue in metabolic syndrome, aging, and cancer cachexia. Front Med. 2018; 12:130–8.
https://doi.org/10.1007/s11684-017-0555-2
PMID:29119382

6. Cypess AM, Lehman S, Williams G, Tal I, Rodman D, Goldfine AB, Kuo FC, Palmer EL, Tseng YH, Doria A, Kolodny GM, Kahn CR. Identification and importance of brown adipose tissue in adult humans. N Engl J Med. 2009; 360:1509–17.
https://doi.org/10.1056/NEJMoa0810780
PMID:19357406

7. van Marken Lichtenbelt WD, Vanhommerig JW, Smulders NM, Drossaerts JM, Kemerink GJ, Bouvy ND, Schrauwen P, Teule GJ. Cold-activated brown adipose tissue in healthy men. N Engl J Med. 2009; 360:1500–8.
https://doi.org/10.1056/NEJMoa0808718
PMID:19357405

8. Ouellet V, Labbé SM, Blondin DP, Phoenix S, Guérin B, Haman F, Turcotte EE, Richard D, Carpentier AC. Brown adipose tissue oxidative metabolism contributes to energy expenditure during acute cold exposure in humans. J Clin Invest. 2012; 122:545–52.
https://doi.org/10.1172/JCI60433
PMID:22269323

9. Blondin DP, Labbé SM, Phoenix S, Guérin B, Turcotte ÉE, Richard D, Carpentier AC, Haman F. Contributions of white and brown adipose tissues and skeletal muscles to acute cold-induced metabolic responses in healthy men. J Physiol. 2015; 593:701–14.
https://doi.org/10.1113/jphysiol.2014.283598
PMID:25384777

10. Bartelt A, Bruns OT, Reimer R, Hohenberg H, Ittrich H, Peldschus K, Kaul MG, Tromsdorf UI, Weller H, Waurisch C, Eychmüller A, Gordts PL, Rinninger F, et al. Brown adipose tissue activity controls triglyceride clearance. Nat Med. 2011; 17:200–5.
https://doi.org/10.1038/nm.2297
PMID:21258337

11. Berbée JF, Boon MR, Khedoe PP, Bartelt A, Schlein C, Worthmann A, Kooijman S, Hoeke G, Mol IM, John C, Jung C, Vazirpanah N, Brouwers LP, et al. Brown fat activation reduces hypercholesterolaemia and protects from atherosclerosis development. Nat Commun. 2015; 6:6356.
https://doi.org/10.1038/ncomms7356
PMID:25754609

12. Becher T, Palanisamy S, Kramer DJ, Eljalby M, Marx SJ, Wibmer AG, Butler SD, Jiang CS, Vaughan R, Schöder H, Mark A, Cohen P. Brown adipose tissue is associated with cardiometabolic health. Nat Med. 2021; 27:58–65.
https://doi.org/10.1038/s41591-020-1126-7
PMID:33398160

13. Herz CT, Kulterer OC, Prager M, Schmöltzer C, Langer FB, Prager G, Marculescu R, Kautzky-Willer A, Hacker M, Haug AR, Kiefer FW. Active Brown Adipose Tissue is Associated With a Healthier Metabolic Phenotype in Obesity. Diabetes. 2021; 71:93–103.
https://doi.org/10.2337/db21-0475
PMID:34957487

14. Kroon J, Schilperoort M, In Het Panhuis W, van den Berg R, van Doeselaar L, Verzijl CRC, van Trigt N, Mol IM, Sips HHC, van den Heuvel JK, Koorneef LL, van der Sluis RJ, Fenzl A, et al. A physiological glucocorticoid rhythm is an important regulator of brown adipose tissue function. Mol Metab. 2021; 47:101179.
https://doi.org/10.1016/j.molmet.2021.101179
PMID:33548499

15. Lee P, Bova R, Schofield L, Bryant W, Dieckmann W, Slattery A, Govendir MA, Emmett L, Greenfield JR. Brown Adipose Tissue Exhibits a Glucose-Responsive Thermogenic Biorhythm in Humans. Cell Metab. 2016; 23:602–9.
https://doi.org/10.1016/j.cmet.2016.02.007
PMID:26972823

16. Søberg S, Löfgren J, Philipsen FE, Jensen M, Hansen AE, Ahrens E, Nystrup KB, Nielsen RD, Sølling C, Wedell-Neergaard AS, Berntsen M, Loft A, Kjær A, et al. Altered brown fat thermoregulation and enhanced cold-induced thermogenesis in young, healthy, winter-swimming men. Cell Rep Med. 2021; 2:100408.
https://doi.org/10.1016/j.xcrm.2021.100408
PMID:34755128

17. van den Berg R, Kooijman S, Noordam R, Ramkisoensing A, Abreu-Vieira G, Tambyrajah LL, Dijk W, Ruppert P, Mol IM, Kramar B, Caputo R, Puig LS, de Ruiter EM, et al. A Diurnal Rhythm in Brown Adipose Tissue Causes Rapid Clearance and Combustion of Plasma Lipids at Wakening. Cell Rep. 2018; 22:3521–33.
https://doi.org/10.1016/j.celrep.2018.03.004
PMID:29590620

18. van der Veen DR, Shao J, Chapman S, Leevy WM, Duffield GE. A diurnal rhythm in glucose uptake in brown adipose tissue revealed by in vivo PET-FDG imaging. Obesity (Silver Spring). 2012; 20:1527–9.
https://doi.org/10.1038/oby.2012.78
PMID:22447290

19. Matsushita M, Nirengi S, Hibi M, Wakabayashi H, Lee SI, Domichi M, Sakane N, Saito M. Diurnal variations of brown fat thermogenesis and fat oxidation in humans. Int J Obes (Lond). 2021; 45:2499–505.
https://doi.org/10.1038/s41366-021-00927-x
PMID:34341470

20. Zadelaar AS, Boesten LS, Jukema JW, van Vlijmen BJ, Kooistra T, Emeis JJ, Lundholm E, Camejo G, Havekes LM. Dual PPARalpha/gamma agonist tesaglitazar reduces atherosclerosis in insulin-resistant and hypercholesterolemic ApoE*3Leiden mice. Arterioscler Thromb Vasc Biol. 2006; 26:2560–6.
https://doi.org/10.1161/01.ATV.0000242904.34700.66
PMID:16931788

21. Westerterp M, van der Hoogt CC, de Haan W, Offerman EH, Dallinga-Thie GM, Jukema JW, Havekes LM, Rensen PC. Cholesteryl ester transfer protein decreases high-density lipoprotein and severely aggravates atherosclerosis in APOE*3-Leiden mice. Arterioscler Thromb Vasc Biol. 2006; 26:2552–9.
https://doi.org/10.1161/01.ATV.0000243925.65265.3c
PMID:16946130

22. Korach-André M, Archer A, Barros RP, Parini P, Gustafsson JÅ. Both liver-X receptor (LXR) isoforms control energy expenditure by regulating brown adipose tissue activity. Proc Natl Acad Sci U S A. 2011; 108:403–8.
https://doi.org/10.1073/pnas.1017884108
PMID:21173252

23. Cannon B, Nedergaard J. Brown adipose tissue: function and physiological significance. Physiol Rev. 2004; 84:277–359.
https://doi.org/10.1152/physrev.00015.2003
PMID:14715917

24. van Eenige R, In Het Panhuis W, Schönke M, Jouffe C, Devilee TH, Siebeler R, Streefland TCM, Sips HCM, Pronk ACM, Vorderman RHP, Mei H, van Klinken JB, van Weeghel M, et al. Angiopoietin-like 4 governs diurnal lipoprotein lipase activity in brown adipose tissue. Mol Metab. 2022; 60:101497.
https://doi.org/10.1016/j.molmet.2022.101497
PMID:35413480

25. Held NM, Buijink MR, Elfrink HL, Kooijman S, Janssens GE, Luyf ACM, Pras-Raves ML, Vaz FM, Michel S, Houtkooper RH, van Weeghel M. Aging selectively dampens oscillation of lipid abundance in white and brown adipose tissue. Sci Rep. 2021; 11:5932.
https://doi.org/10.1038/s41598-021-85455-4
PMID:33723320

26. Sutton GM, Ptitsyn AA, Floyd ZE, Yu G, Wu X, Hamel K, Shah FS, Centanni A, Eilertsen K, Kheterpal I, Newman S, Leonardi C, Freitas MA, et al. Biological

aging alters circadian mechanisms in murine adipose tissue depots. Age (Dordr). 2013; 35:533–47. https://doi.org/10.1007/s11357-012-9389-7 PMID:22411258

27. Hoffman JM, Valencak TG. Sex differences and aging: Is there a role of brown adipose tissue? Mol Cell Endocrinol. 2021; 531:111310. https://doi.org/10.1016/j.mce.2021.111310 PMID:33989715

28. Yoneshiro T, Aita S, Matsushita M, Kayahara T, Kameya T, Kawai Y, Iwanaga T, Saito M. Recruited brown adipose tissue as an antiobesity agent in humans. J Clin Invest. 2013; 123:3404–8. https://doi.org/10.1172/JCI67803 PMID:23867622

29. Khedoe PP, Hoeke G, Kooijman S, Dijk W, Buijs JT, Kersten S, Havekes LM, Hiemstra PS, Berbée JF, Boon MR, Rensen PC. Brown adipose tissue takes up plasma triglycerides mostly after lipolysis. J Lipid Res. 2015; 56:51–9. https://doi.org/10.1194/jlr.M052746 PMID:25351615

30. Schilperoort M, Hoeke G, Kooijman S, Rensen PC. Relevance of lipid metabolism for brown fat visualization and quantification. Curr Opin Lipidol. 2016; 27:242–8. https://doi.org/10.1097/MOL.0000000000000296 PMID:27023630

31. Paalvast Y, Gerding A, Wang Y, Bloks VW, van Dijk TH, Havinga R, Willems van Dijk K, Rensen PCN, Bakker BM, Kuivenhoven JA, Groen AK. Male apoE*3-Leiden.CETP mice on high-fat high-cholesterol diet exhibit a biphasic dyslipidemic response, mimicking the changes in plasma lipids observed through life in men. Physiol Rep. 2017; 5:e13376. https://doi.org/10.14814/phy2.13376 PMID:29038350

32. Yu P, Yuan R, Yang X, Qi Z. Adipose tissue, aging, and metabolism. Curr Opin Endocr Metab Res. 2019; 5:11–20. https://doi.org/10.1016/j.coemr.2019.02.003

33. Yuan RK, Zitting KM, Wang W, Buxton OM, Williams JS, Duffy JF, Czeisler CA. Fasting blood triglycerides vary with circadian phase in both young and older people. Physiol Rep. 2020; 8:e14453. https://doi.org/10.14814/phy2.14453 PMID:32519460

34. Adamovich Y, Aviram R, Asher G. The emerging roles of lipids in circadian control. Biochim Biophys Acta. 2015; 1851:1017–25. https://doi.org/10.1016/j.bbalip.2014.11.013 PMID:25483623

35. Li Y, Ma J, Yao K, Su W, Tan B, Wu X, Huang X, Li T, Yin Y, Tosini G, Yin J. Circadian rhythms and obesity: Timekeeping governs lipid metabolism. J Pineal Res. 2020; 69:e12682. https://doi.org/10.1111/jpi.12682 PMID:32656907

36. Dijk W, Heine M, Vergnes L, Boon MR, Schaart G, Hesselink MK, Reue K, van Marken Lichtenbelt WD, Olivecrona G, Rensen PC, Heeren J, Kersten S. ANGPTL4 mediates shuttling of lipid fuel to brown adipose tissue during sustained cold exposure. Elife. 2015; 4:e08428. https://doi.org/10.7554/eLife.08428 PMID:26476336

37. Grootendorst J, Enthoven L, Dalm S, de Kloet ER, Oitzl MS. Increased corticosterone secretion and early-onset of cognitive decline in female apolipoprotein E-knockout mice. Behav Brain Res. 2004; 148:167–77. https://doi.org/10.1016/s0166-4328(03)00188-8 PMID:14684257

38. Pilorz V, Steinlechner S, Oster H. Age and oestrus cycle-related changes in glucocorticoid excretion and wheel-running activity in female mice carrying mutations in the circadian clock genes Per1 and Per2. Physiol Behav. 2009; 96:57–63. https://doi.org/10.1016/j.physbeh.2008.08.010 PMID:18786554

39. Bahler L, Verberne HJ, Admiraal WM, Stok WJ, Soeters MR, Hoekstra JB, Holleman F. Differences in Sympathetic Nervous Stimulation of Brown Adipose Tissue Between the Young and Old, and the Lean and Obese. J Nucl Med. 2016; 57:372–7. https://doi.org/10.2967/jnumed.115.165829 PMID:26609175

40. Van Cauter E, Leproult R, Kupfer DJ. Effects of gender and age on the levels and circadian rhythmicity of plasma cortisol. J Clin Endocrinol Metab. 1996; 81:2468–73. https://doi.org/10.1210/jcem.81.7.8675562 PMID:8675562

41. Graja A, Schulz TJ. Mechanisms of aging-related impairment of brown adipocyte development and function. Gerontology. 2015; 61:211–7. https://doi.org/10.1159/000366557 PMID:25531079

42. Froy O, Garaulet M. The Circadian Clock in White and Brown Adipose Tissue: Mechanistic, Endocrine, and Clinical Aspects. Endocr Rev. 2018; 39:261–73. https://doi.org/10.1210/er.2017-00193 PMID:29490014

43. Hasan N, Nagata N, Morishige JI, Islam MT, Jing Z, Harada KI, Mieda M, Ono M, Fujiwara H, Daikoku T,

Fujiwara T, Maida Y, Ota T, et al. Brown adipocyte-specific knockout of Bmal1 causes mild but significant thermogenesis impairment in mice. Mol Metab. 2021; 49:101202.
https://doi.org/10.1016/j.molmet.2021.101202
PMID:33676029

44. Oh-ishi S, Kizaki T, Toshinai K, Haga S, Fukuda K, Nagata N, Ohno H. Swimming training improves brown-adipose-tissue activity in young and old mice. Mech Ageing Dev. 1996; 89:67–78.
https://doi.org/10.1016/0047-6374(96)01727-7
PMID:8844640

45. Corrales P, Vivas Y, Izquierdo-Lahuerta A, Horrillo D, Seoane-Collazo P, Velasco I, Torres L, Lopez Y, Martínez C, López M, Ros M, Obregon MJ, Medina-Gomez G. Long-term caloric restriction ameliorates deleterious effects of aging on white and brown adipose tissue plasticity. Aging Cell. 2019; 18:e12948.
https://doi.org/10.1111/acel.12948
PMID:30920127

46. Scarpace PJ, Tse C, Matheny M. Thermoregulation with age: restoration of beta(3)-adrenergic responsiveness in brown adipose tissue by cold exposure. Proc Soc Exp Biol Med. 1996; 211:374–80.
https://doi.org/10.3181/00379727-211-43983
PMID:8618944

47. Sellayah D, Sikder D. Orexin restores aging-related brown adipose tissue dysfunction in male mice. Endocrinology. 2014; 155:485–501.
https://doi.org/10.1210/en.2013-1629
PMID:24248466

48. Geldenhuys WJ, Lin L, Darvesh AS, Sadana P. Emerging strategies of targeting lipoprotein lipase for metabolic and cardiovascular diseases. Drug Discov Today. 2017; 22:352–65.
https://doi.org/10.1016/j.drudis.2016.10.007
PMID:27771332

49. Rensen PC, van Dijk MC, Havenaar EC, Bijsterbosch MK, Kruijt JK, van Berkel TJ. Selective liver targeting of antivirals by recombinant chylomicrons--a new therapeutic approach to hepatitis B. Nat Med. 1995; 1:221–5.
https://doi.org/10.1038/nm0395-221
PMID:7585037

50. Cardiff RD, Miller CH, Munn RJ. Manual hematoxylin and eosin staining of mouse tissue sections. Cold Spring Harb Protoc. 2014; 2014:655–8.
https://doi.org/10.1101/pdb.prot073411
PMID:24890205

51. Davies BS, Beigneux AP, Barnes RH 2nd, Tu Y, Gin P, Weinstein MM, Nobumori C, Nyrén R, Goldberg I, Olivecrona G, Bensadoun A, Young SG, Fong LG. GPIHBP1 is responsible for the entry of lipoprotein lipase into capillaries. Cell Metab. 2010; 12:42–52.
https://doi.org/10.1016/j.cmet.2010.04.016
PMID:20620994
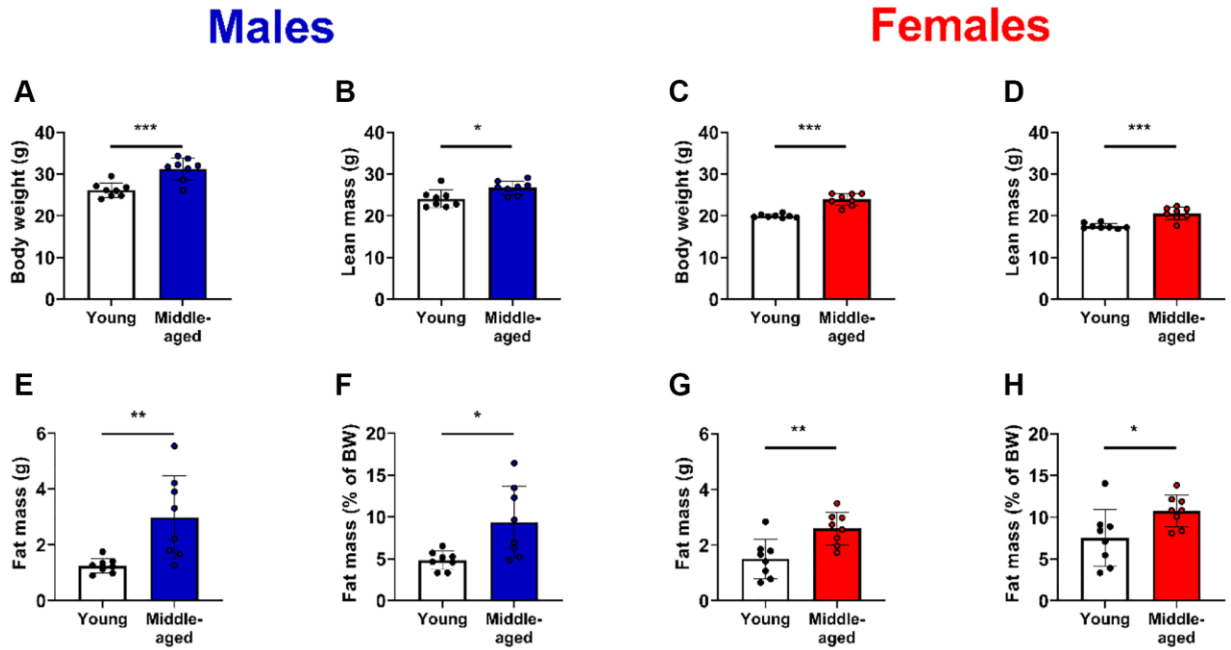
Supplementary Figure 1. Body composition and aging. Young (12 weeks old) and middle-aged (52 weeks old) male (left panels in blue) and female (right panels in red) C57BL/6J mice were compared (n = 8 mice/group). (**A**, **C**) body weight, (**B**, **D**) lean mass, and (**E**, **G**) fat mass from which (**F**, **H**) the percentage of fat mass relative to body weight (BW) was calculated. Bar graphs represent means ± SD. $^*p < 0.05$; $^{**}p < 0.01$; $^{***}p < 0.001$, according to unpaired t-test.
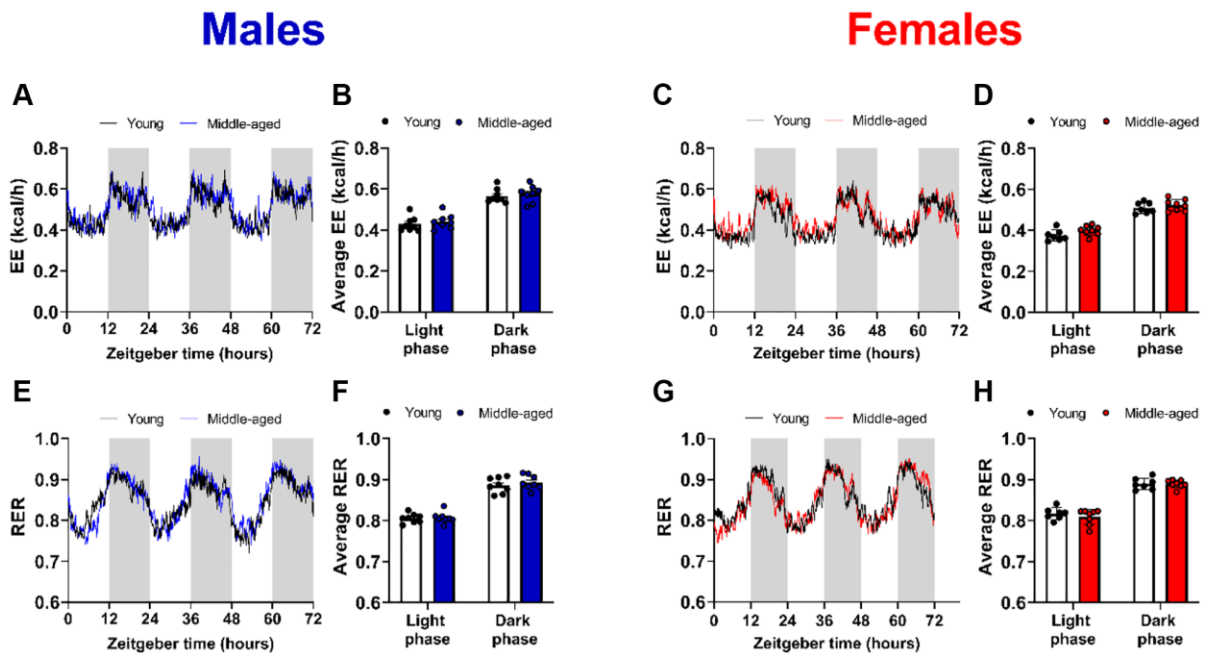
Supplementary Figure 2. Energy expenditure and respiratory exchange ratio during aging. Young (12 weeks old) and middle-aged (52 weeks old) male (left panels in blue) and female (right panels in red) C57BL/6J mice (n = 8 mice/group) were single-housed in metabolic cages for continuous measurements of O_2 consumption and CO_2 production, from which (**A–D**) energy expenditure (EE) and (**E–H**) respiratory exchange ratio (RER) were calculated. Bar graphs represent means ± SD. No significant differences were observed according to unpaired t-test and two-way ANOVA and following Šídák's multiple-comparison test.
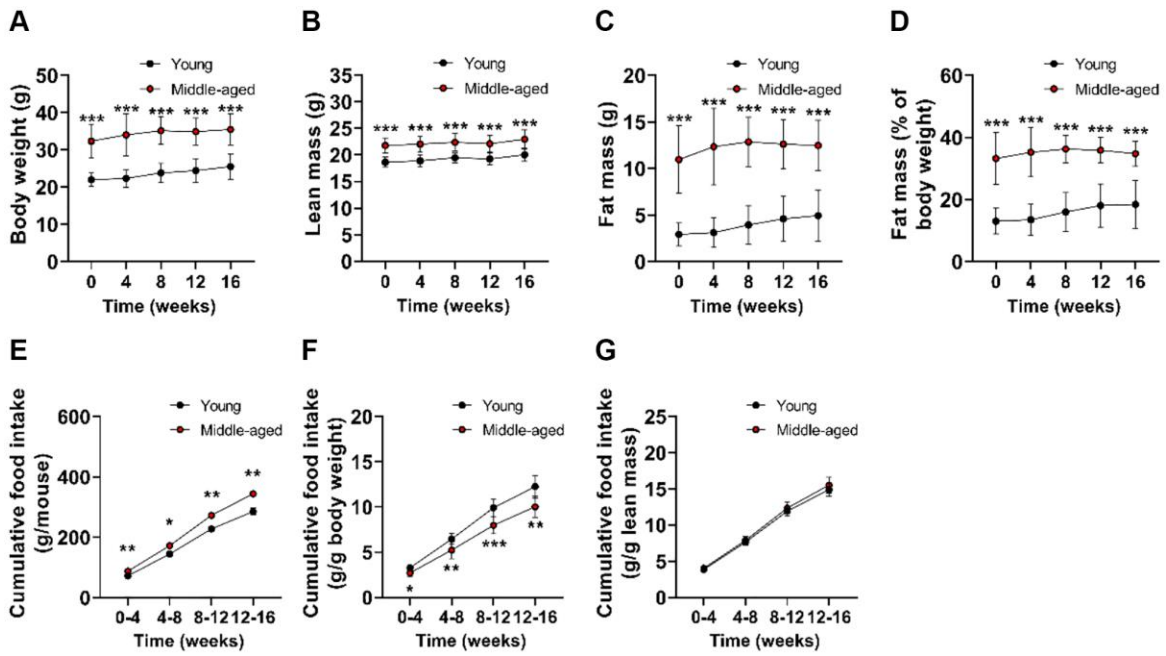
Supplementary Figure 3. Body composition and aging. Young (11–15 weeks old) and middle-aged (51–55 weeks old) female APOE*3-Leiden.CETP mice (*n* = 15–16 mice/group) were followed for 16 weeks to monitor (**A**) body weight, (**B**) fat mass, and (**C**) lean mass. (**D**) Fat mass was additionally expressed as a percentage of body weight. (**E**) Cumulative food intake per cage was calculated per 4 weeks, and corrected for (**F**) body weight and (**G**) lean mass (*n* = 16 mice/group). Data points on curves represent means ± SD. $^*p < 0.05$, $^{**}p < 0.01$, $^{***}p < 0.001$, according to two-way ANOVA and Tukey's multiple-comparison test.
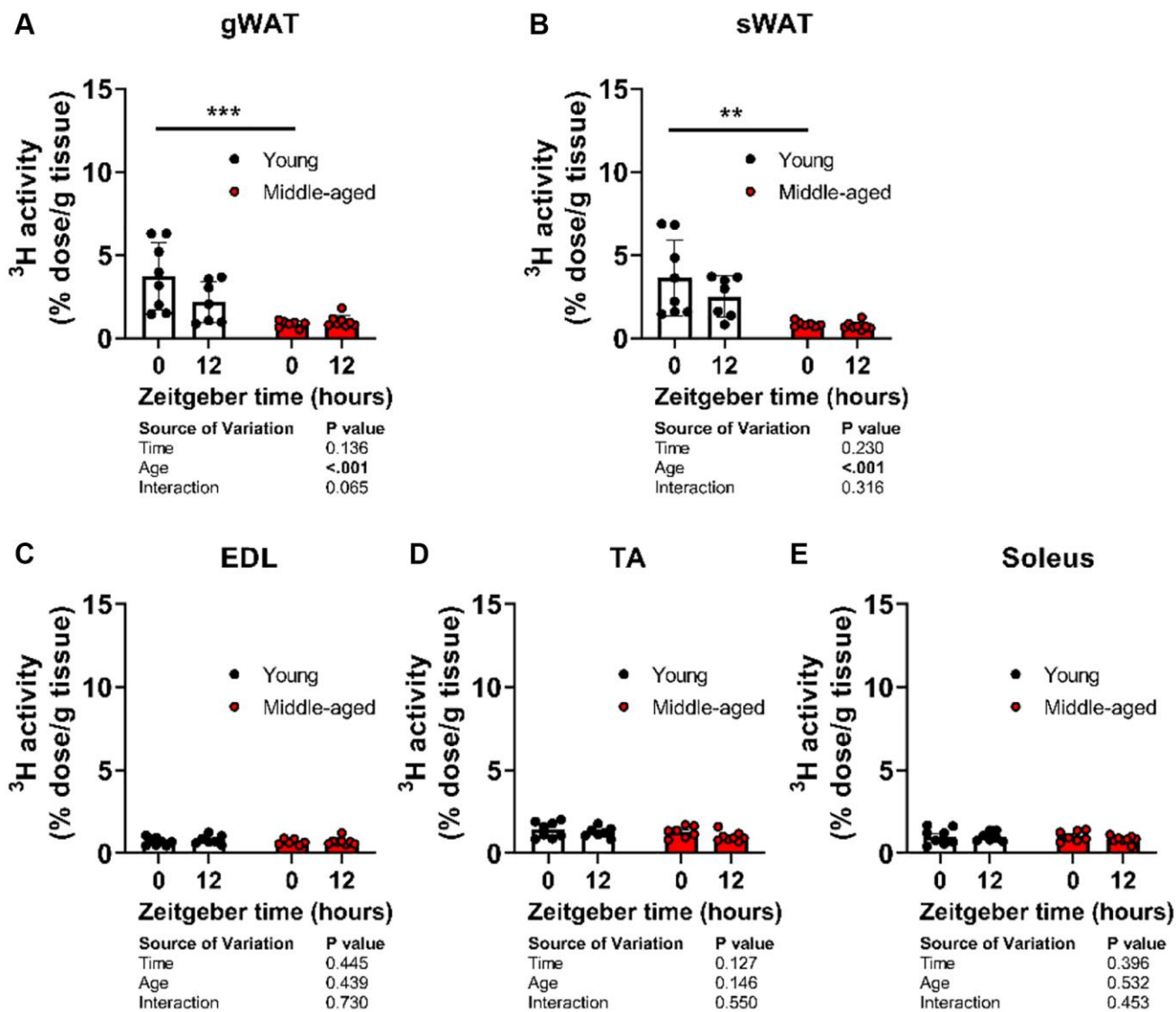
Supplementary Figure 4. Triglyceride-derived fatty acid uptake by white adipose tissues and skeletal muscles during aging. Young (27–31 weeks old) and middle-aged (67-71 weeks old) female APOE*3-Leiden.CETP mice were injected with triglyceride-rich lipoprotein-like particles double-labeled with glycerol tri[^{3}H]oleate and [^{14}C]cholesteryl oleate at *Zeitgeber* Time 0 and 12 (n = 6–8 mice/group/time point) to assess [^{3}H]oleate uptake by (**A**) gonadal white adipose tissue (gWAT), (**B**) subcutaneous WAT (sWAT), (**C**) extensor digitorum longus (EDL), (**D**) tibialis anterior (TA), and (**E**) soleus. Bar graphs represent means ± SD. **$^{**}p < 0.01$; $^{***}p < 0.001$, according to two-way ANOVA and following Tukey's multiple-comparison test.

Supplementary Table

Supplementary Table 1. Primer list.

Gene	Primer sequence
Acc	Forward AGATGGCCGATCAGTACGTC
	Reverse GGGGACCTAGGAAAGCAATC
Acox	Forward TATGGGATCAGCCAGAAAGG
	Reverse ACAGAGCCAAGGGTCACATC
Angptl4	Forward GGAAAGAGGCTTCCCAAGAT
	Reverse TCCCAGGACTGGTTGAAGTC
β-actin	Forward AACCGTGAAAAGATGACCCAGAT
	Reverse CACAGCCTGGATGGCTACGTA
Bmal1	Forward ATGCCAAGACTGGACTTCCG
	Reverse TGCAGAAGCTTTTTCGATCTGC
Clock	Forward AGTTAGGGCTGAAAGACGGC
	Reverse GGTGTGGAGGAAGGGTCTGA
Cpt1	Forward GAGACTTCCAACGCATGACA
	Reverse ATGGGTTGGGGGTGATGTAGA
Cry1	Forward AGAGGGCTAGGTCTTCTCGC
	Reverse GTGAGTCTGCTGACTGTCCC
Fasn	Forward GCGCTCCTCGCTTGTCGTCT
	Reverse TAGAGCCCAGCCTTCCATCTCCTG
Lpl	Forward CCCTAAGGACCCCTGAAGAC
	Reverse GGCCCGATACAACCAGTCTA
Lxra	Forward CTGCACGCCTACGTCTCCAT
	Reverse AAGTACGGAGGCTCACCAGCT
Nr1d1	Forward GTGCTTGTCTCTGCAGACCG
	Reverse TTGGTGAAGCGGGAAGTCTC
Per1	Forward ACGGCCAGGTGTCGTGATTA
	Reverse CCCTTCTAGGGGACCACTCA
Srebp1c	Forward AGCCGTGGTGAGAAGCGCAC
	Reverse ACACCAGGTCCTTCAGTGATTTGCT
Ucp1	Forward TCAGGATTGGCCTCTACGAC
	Reverse TGCATTCTGACCTTCACGAC